Int. J. Electrochem. Sci., 8 **(2013)** 7211 - 7222

International Journal of
ELECTROCHEMICAL
SCIENCE
www.electrochemsci.org

Determination of Corrosion Type by Wavelet-Based Fractal Dimension from Electrochemical Noise

Xuehui Wang[1, 2], *Jihui Wang*[1,2,3,*] , *Congwei Fu*[2], *Yingkun Gao*[2]

[1] State Key Laboratory of Hyraulic Engineering Simulation and Safety, Tianjin University, Tianjin 300072, R R China
[2] Tianjin Key Laboratory of Composite and Functional Materials, School of Materials Science and Engineering, Tianjin University, Tianjin 300072, P R China
[3] School of Materials Science and Engineering, Tianjin University, Weijin Road 92#, Tianjin 300072, P R China.
[*]E-mail: jhwang@tju.edu.cn

Received: 16 January 2013 / *Accepted:* 18 February 2013 / *Published:* 1 May 2013

The corrosion process of general corrosion, passivation, intergranular corrosion, pitting corrosion and crack propagation during stress corrosion cracking of 304 austenitic stainless steels were investigated by electrochemical noise technique. The wavelet based fractal dimension *D* was calculated by using discrete wavelet transform for corrosion-types identification. The results showed that the fractal dimensions of 304 stainless steels under general corrosion and passivation were larger than 2, which implied that corrosion behaviors occurred uniformly over the whole two-dimensional areas, and the *D* value of general corrosion (*D*=2.411) was slightly larger than that of passivation (*D*=2.242). Whereas the fractal dimensions of pitting corrosion and crack propagation were much lower than 2, which indicated that localized corrosion occurred, and the *D* value of pitting corrosion (*D*=1.540) was larger than that of crack propagation (*D*=1.001). Besides, the fractal dimension of intergranular corrosion (*D*=1.970) was in the vicinity to 2, which illustrated that intergranular corrosion occurred more uniformly over the electrode surface than pitting corrosion, whereas more locally than general corrosion. By correlated with the corrosion process and corroded surface morphology of 304 stainless steels, the fractal dimension *D* can be selected to distinguish corrosion types and evaluate the localized degree of corrosion.

Keywords: Electrochemical noise; wavelets; fractal dimension; corrosion type

1. INTRODUCTION

Austenitic stainless steels are widely used in power, chemical, petrochemical and nuclear industries because of their excellent resistance to general corrosion. However, stainless steels are very

easier to suffer from localized corrosion, such as pitting corrosion, intergranular corrosion and environmental induced cracking, particularly in nuclear and petrochemical applications.[1, 2]

Several electrochemical techniques, such as polarization curve,[3] electrochemical impedance spectroscopy[4] and dynamic electrochemical impedance spectroscopy techniques,[5] have been used to determine the corrosion behavior of stainless steels. Nevertheless, the perturbation signals applied in these deterministic techniques may lead to the alteration of corrosion process. In contrast, electrochemical noise (EN) technique is referred to the only non-intrusive technique which consists of fluctuations in the potential and current generated spontaneously by corrosion processes.[6-9] To analyze the EN data, statistical and/or Fourier spectral methods has conventionally been used. The average charge q in each event, frequency of events f_n, and parameters of S_E and S_G have been used to evaluate the corrosion type; while the standard deviation of current or potential (σ_I , σ_V), noise resistance R_n are always used to evaluate the corrosion rate.[10-13]

It is well known that EN which originates from the corrosion process is generally non-stationary and nonlinear in character. However, the commonly used EN analysis methods above are developed under the assumption that EN is stationary. Therefore, there is a limitation of these analytical methods for nonlinear phenomena.[6, 14] Considering these, chaos analysis is then carried out to determine the characteristics of nonlinear corrosion phenomena, and the correlation dimension and fractal parameter are proposed to evaluate different types of corrosion.[6, 15, 16]

Wavelet transform is a relatively useful mathematical tool used to supplement conventional Fourier analysis, and suitable for the time-frequency analysis of non-stationary signals.[17-19] It has also been successfully used in processing EN signals.[20-22] Several wavelet-based parameters, such as energy distribution plot (EDP), standard deviation of partial signal plot,[23] wavelet based noise resistance,[24] have been defined to describe the corrosion process. Considering the fractal nature of corrosion processes and corresponding EN signals, wavelet based fractal analysis is also proposed to understand the EN character and corrosion process,[7, 17, 25] and the persistence and/or stationary characteristics of EN signals are generally analyzed. However, there is few literature concerning about the relationship between the wavelet based fractal dimension and the corroded morphology of metals.

The objective of this paper was to distinguish the corrosion types of 304 stainless steels (SS) by using EN technique: the general corrosion, passivation, intergranular corrosion, pitting corrosion and stress corrosion cracking (SCC). The EDP and the fractal dimension D calculated by means of discrete wavelet transform were investigated. The relationship among the wavelet based fractal dimension D, the corrosion mechanisms and corroded surface morphology were discussed.

2. EXPERIMENTAL

2.1 Electrochemical noise measurement

304 SS was used as the test material for this experiment, its chemical composition was shown as follows (in mass fraction): 0.080%C, 18.0%-20.0%Cr, 8.00%-11.0%Ni, 2.0%Mn, 1.0%Si, 0.045%P, 0.03%S and Fe balance.

A three-electrode system was used for EN tests. Two nominally identical 304 SS (10mm×10mm×2mm) were made as working electrode and counter electrode, and a saturated calomel electrode (SCE) with a Luggin capillary tube and a porous tip was used as reference electrode. The surface of all the working electrodes with an exposed area of 1 cm^2 was abraded with silicon carbide paper (from 400# to 2000#) and polished. The EN tests were carried out at 25±3 °C by using a VersaSTAT 4 electrochemical workstation with zero resistance ammeter (ZRA) mode and a sampling frequency (f_s) of 2Hz.

For general corrosion, passivation and pitting corrosion, 304 SS treated by solid solution were immersed in 5%H_2SO_4 (wt%), 0.1%NaOH(wt%) and 0.1mol/L $FeCl_3$ solutions for 5 hours, respectively[6, 26] As for intergranular corrosion, heavy sensitized 304 stainless steel (sensitized at 650 °C for 14 h[27]) were immersed in 0.5mol/L H_2SO_4+ 0.01mol/L KSCN solution for 1 hour.[28] For the stress corrosion cracks propagating process, a pre-cracked specimen (120mm×15mm×2mm) with a crack length of 1.3202 mm was prepared by using fatigue testing machine (INSTRON8562A). And then the slow strain rate tensile method with a strain rate of 1×10^{-5} $s^{-1}$was applied to propagate the crack in 0.5mol/L $Na_2S_2O_3$ solution for 2 hours.

After EN tests, the corroded surface was observed by BX41RF-LED optical microscope. At least 4-5 specimens of each corrosion type test were evaluated in each experiment in order to guarantee the reproducibility of EN data.

2.2 wavelet-based fractal analysis

It was reported that if the capacitively coupled main interference was negligible, the electrochemical potential noise (EPN) was not affected by solution resistance [29]. Thus it's reliable to use EPN for corrosion systems identification in different electrolytic solutions.[6, 13, 30, 31] Consequently, by using the wavelet transform technique based on orthogonal db2 wavelet,[7] the collected EPN data were decomposed to seven levels (*d*1-*d*7, and *s*7). As the approximation signal *s*7 had the elimination effect on holistic potential evolution, the original data did not need to remove the direct current (DC) component.[32] Then, the fraction of energy associated with each detail crystal E_j^d was calculated as follows:

$$E_j^d = \frac{1}{E}\sum_{n=1}^{N/2^j} d_{j,n}^2 \ (j=1, 2, \ldots, 7)$$

where *d* was the detail crystal and *N* was the total number of data points for each recording run. *E* was the total energy, which equaled to the sum of seven detailed crystals (*d*1-*d*7), discounting the contribution of *s*7 crystal:[32]

$$E = E_1^d + E_2^d + \cdots + E_7^d = \sum_{n=1}^{N/2^1} d_{1,n}^2 + \sum_{n=1}^{N/2^2} d_{2,n}^2 + \cdots + \sum_{n=1}^{N/2^7} d_{7,n}^2$$

The scale range of detailed crystal was listed in Table 1.

Table 1. Frequency and scale range for j = 7 and f_s = 2 Hz.

Crystal name	Frequency range/Hz	Scale range/s
*d*1	2–1	0.5–1
*d*2	1–0.5	1–2
*d*3	0.5–0.25	2–4
*d*4	0.25–0.125	4–8
*d*5	0.125–0.0625	8–16
d6	0.0625–0.0312	16–32
d7	0.0312–0.0156	32–64

For orthonormal discrete wavelet decomposition, the following power law was obeyed:[7, 17]

$$\sigma_j^2 = \frac{\sigma^2}{(2^j)^{-\beta}}$$

Where σ_j^2 was the variance of detail crystal d_j, and could be calculated by the following equation:

$$\sigma_j^2 = \frac{1}{N/2^j - 1} \sum_{n=1}^{N/2^j} (d_{j,k} - d_j)^2 \ (j=1, 2\ldots..7)$$

The slope β was obtained from the plot $\log_2 \sigma_j^2$ versus level j:

$$\log_2 \sigma_j^2 = \beta j + \log_2 \sigma^2$$

Finally, the fractal dimension D was obtained by:

$$D = 2.5 - 0.5\beta$$

A period of 512 s was set for each noise recording run, the EDP and fractal dimension parameter D was calculated between each 30 minutes.

3. RESULTS

3.1 Surface morphology

The surface morphology of 304 SS after EN tests is shown in Fig. 1. General corrosion showed tarnish appearance, the material dissolved uniformly on the whole surface (Fig. 1a). As for passivation, there was hardly any corrosion phenomena occurred on the surface, which indicated that passive film was formed on the metal (Fig. 1b). After intergranular corrosion, there were some steps and ditches on

the grain boundaries (Fig. 1c). For pitting corrosion, several well developed pits with diameter of 10 to 90μm were observed, and the rest surface was not attacked (Fig. 1d).

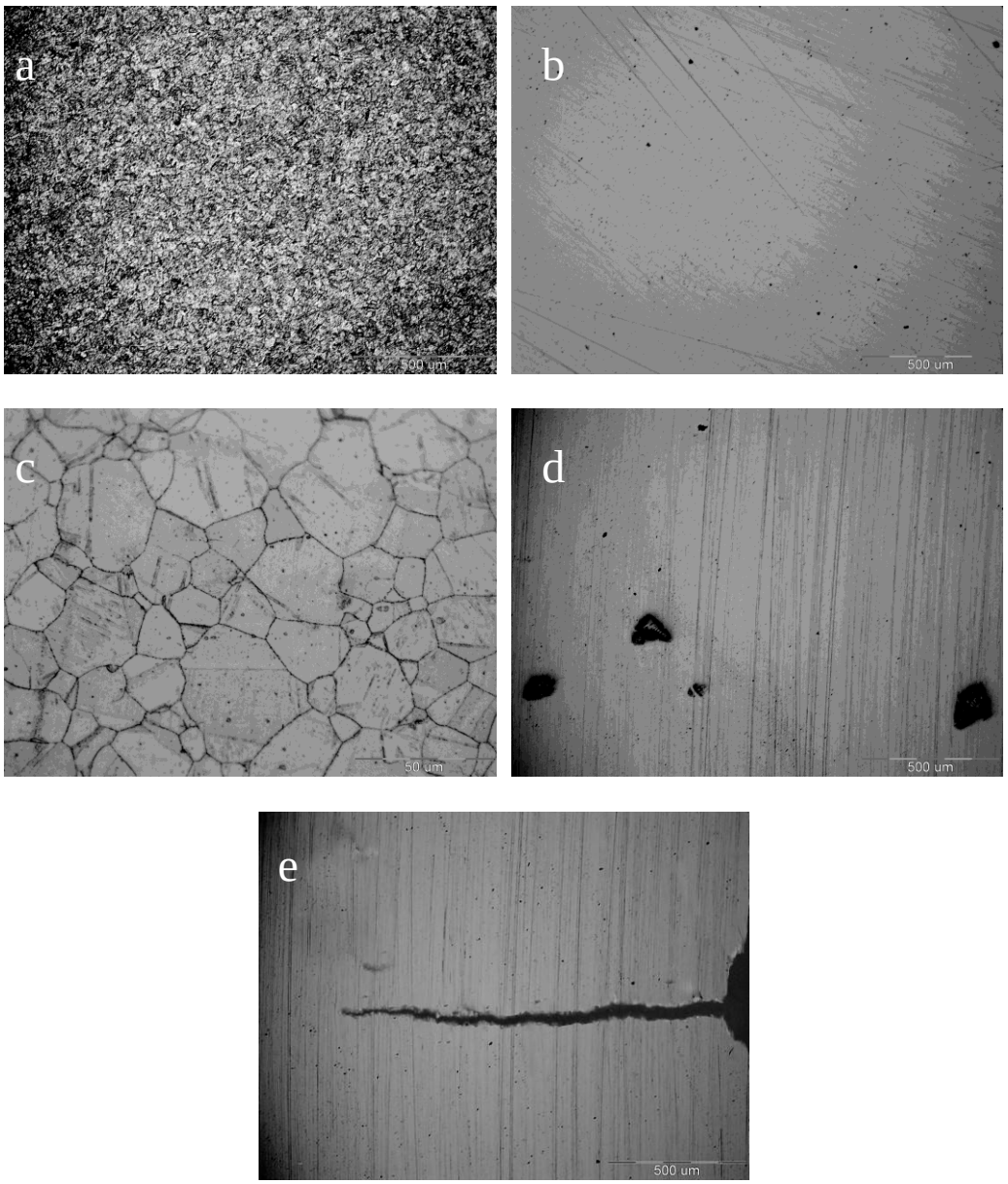

Figure 1. Morphology of 304 SS under (a) general corrosion, (b) passivation, (c) intergranular corrosion, (d) pitting corrosion, (e) crack propagation

After stress corrosion cracking test, the length of pre-crack was propagated from 1.3202mm to 1.4030mm without other changes observed on the surface (Fig. 1e). All these observations indicated that the location of corrosion was changed from whole surface to localized area in the order of general corrosion/passivation, intergranular corrosion, pitting corrosion and crack propagation.

3.2 Electrochemical noise

Fig. 2 is the original EN signals of 304 SS under different corrosion processes after 60 minutes of immersion. During the general corrosion and passivation, the EN signals were in a Gaussian white noise like fluctuations with high frequency (Fig. 2a and 2b). Whereas, the well-defined peaks with relatively low frequency could be observed for pitting corrosion and crack propagating processes (Fig. 2d and 2e). For intergranular corrosion, both Gaussian white noise like fluctuations and well-defined peaks were observed in the EN signals (Fig. 2c). From the characteristics of EN signals, general corrosion or passivation could be discriminated from localized corrosions.

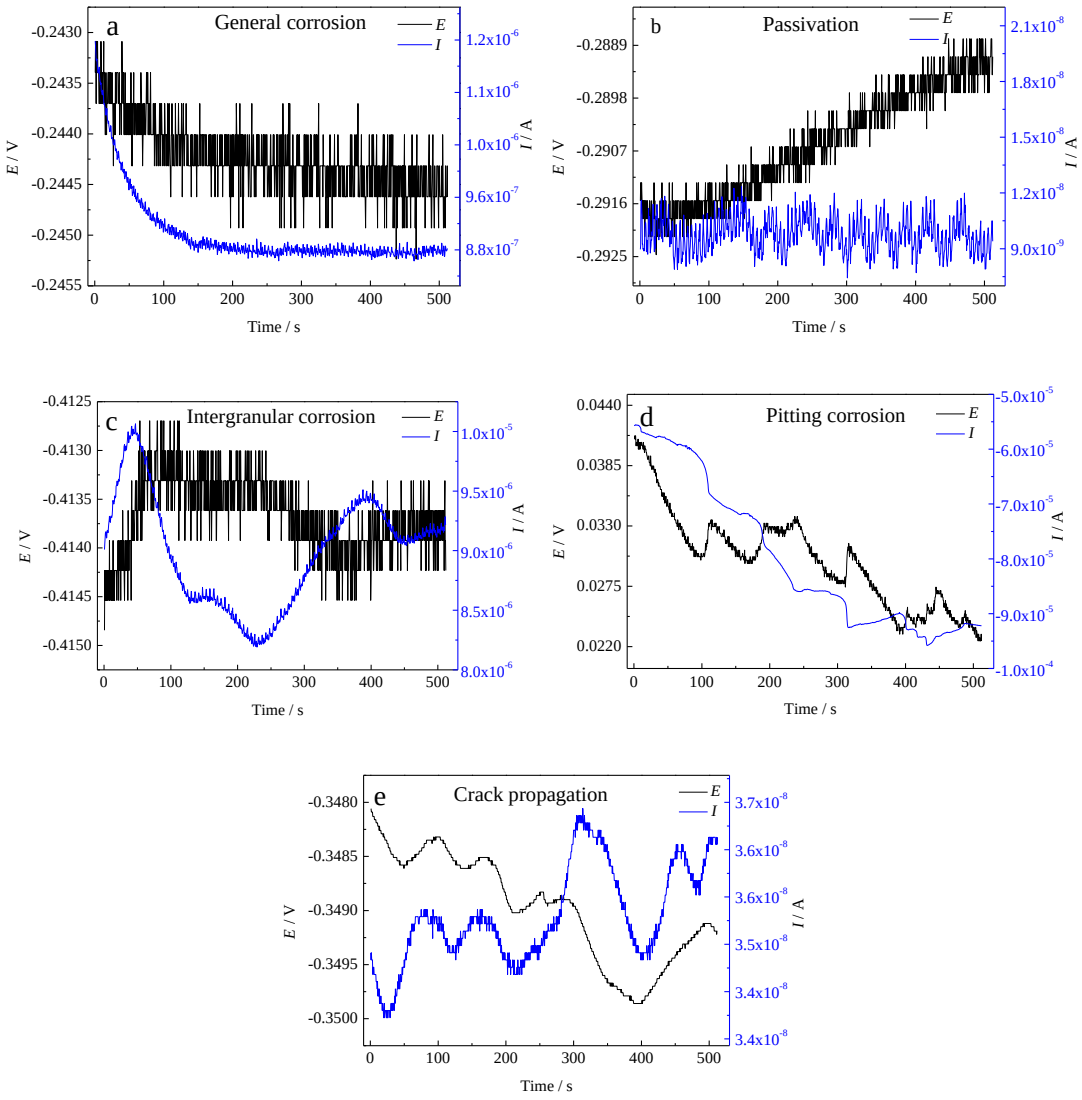

Figure 2. EN signals of 304 SS under different corrosion types (after 60 minutes of immersion): (a) general corrosion, (b) passivation, (c) intergranular corrosion, (d) pitting corrosion, (e) crack propagation

3.3 Energy distribution plot

Fig. 3 shows the EDPs of the seven detail crystals for different corrosion types, corresponding to the potential noise shown in Fig. 2. It could be seen from Fig. 3a and 3b that the maximum relative energy for both general corrosion and passivation was located at the crystal *d*1 coefficient, with a relatively high frequency of 1-2 Hz and a short time width of 0.5-1 s. The peak values of pitting corrosion and crack propagation were defined at the position of *d*7 (Fig. 3d and 3e). They had a relatively low frequency of 0.0312-0.0156 Hz and a long time width of 32-64 s. It indicated that the localized corrosion was a slow process with a low frequency and a long time width. Furthermore, EPN signal for inergranular corrosion in Fig. 2c was composed of two types' fluctuations (i.e. two frequencies), therefore the EDP of inergranular corrosion (Fig. 3c) had two peaks at *d*7and *d*1 crystals respectively. These EDP results were in conformity with the results of EN shown in Fig. 2.

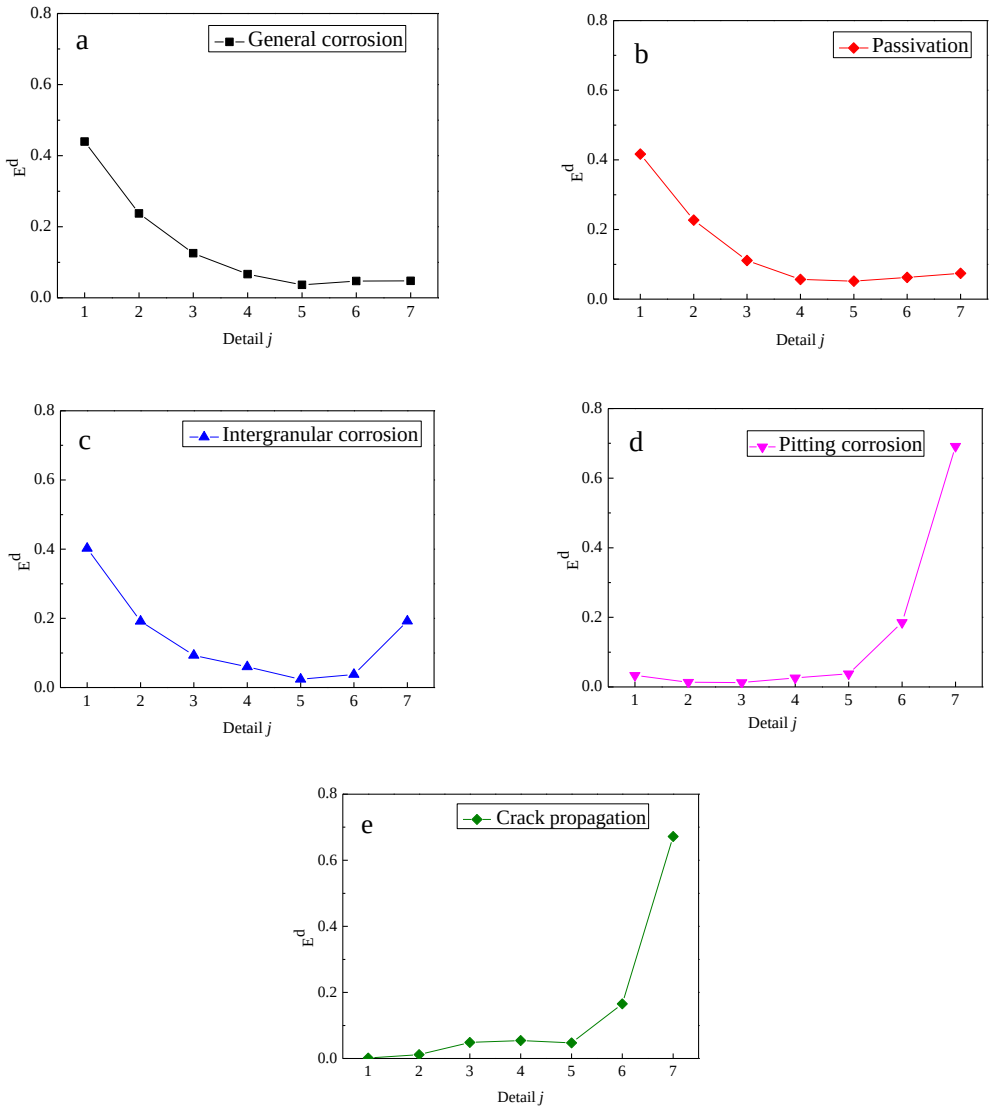

Figure 3. EDPs of the detail coefficient d_j set for different corrosion types (the energy is normalized): (a) general corrosion, (b) passivation, (c) intergranular corrosion, (d) pitting corrosion, (e) crack propagation

3.4 Fractal dimension

The slop β and fractal dimension D are calculated and plotted in Fig. 4 and Fig. 5. The logarithmic plot of details variances σ_j^2 versus level j is shown in Fig.4. It can be seen from Fig. 4 that general corrosion and passivation had low slope values of 0.178 and 0.515 respectively (Fig. 4a and 4b), whereas the intergranular corrosion, pitting corrosion and crack propagation had high slope β values of 1.061, 1.920 and 2.998 respectively (Fig. 4c, 4d and 4e). Considering the fact that the contributions of high-frequency components in EN time series decreased with the increasing of β value[22], more high-frequency components should be observed in the general corrosion and passivation process than in the intergranular, pitting corrosions and crack propagating process. This deduction was in consistent with the observation of EN signals shown in Fig. 2 and EDPs in Fig. 3.

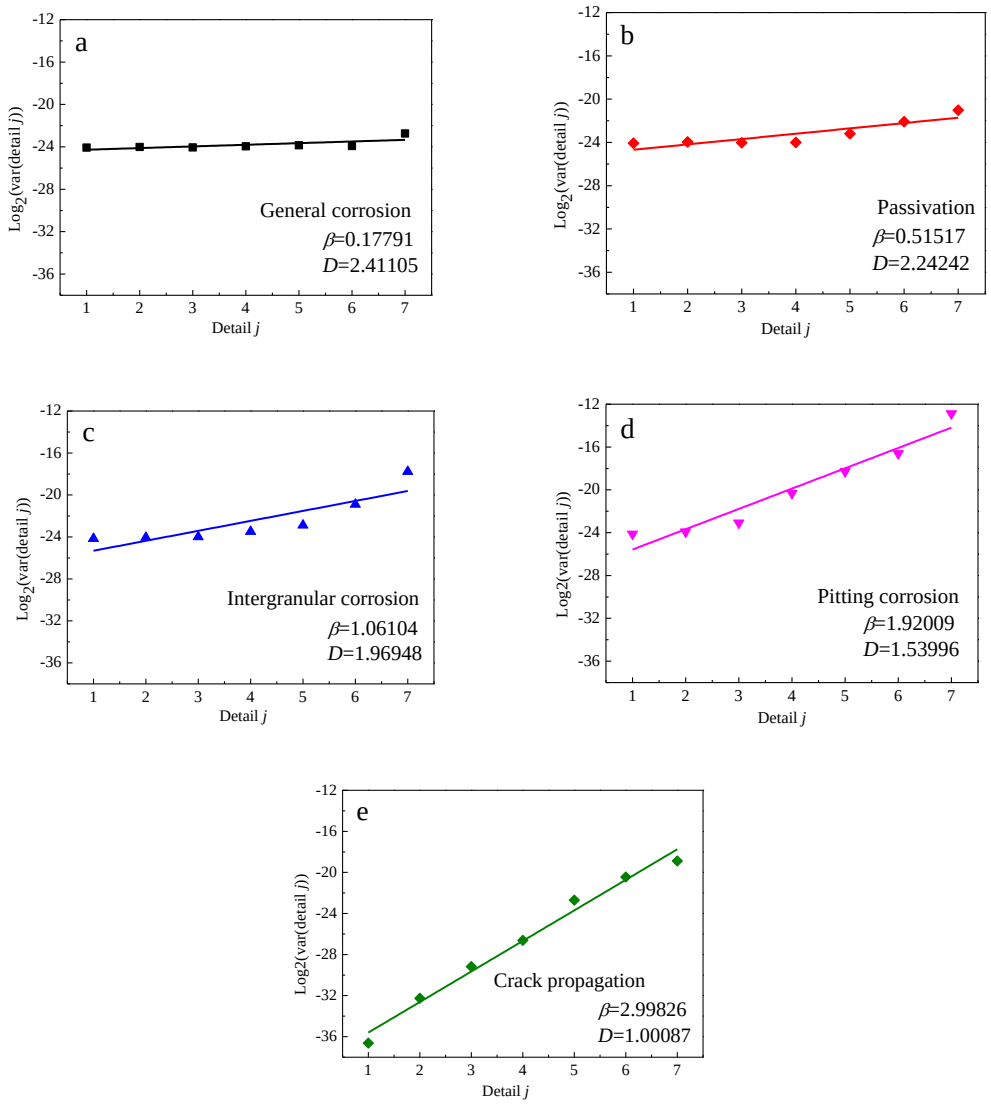

Figure 4. Logarithmic plot of details variances versus detail level j of 304 SS under different corrosion types: (a) general corrosion, (b) passivation, (c) intergranular corrosion, (d) pitting corrosion, (e) crack propagation

Furthermore, it was noticed that the β value, obtained from different EN signals, was increased in the order of general corrosion, passivation, intergranular corrosion, pitting corrosion and crack propagation, as the foresaid order shown in Fig. 1.

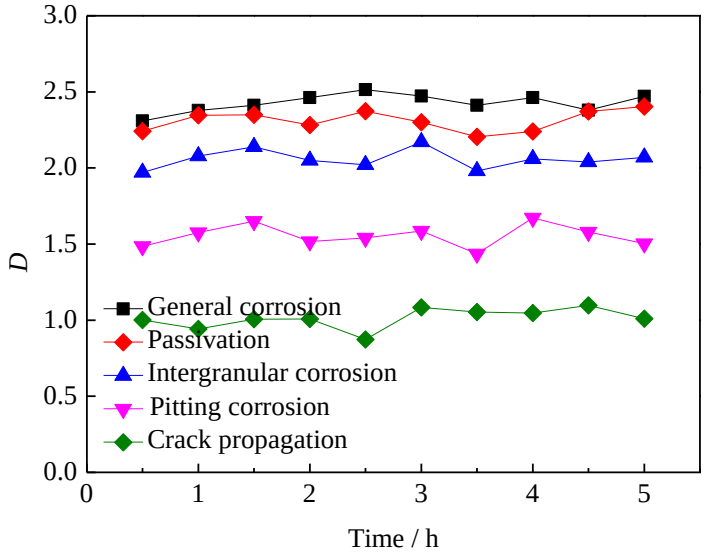

Figure 5. Fractal dimension *D* of 304 SS under different corrosion types: (a) general corrosion, (b) passivation, (c) intergranular corrosion, (d) pitting corrosion, (e) crack propagation

Fig. 5 is the fractal dimension *D* of different corrosion types, calculated from slope β. It was obvious to see that the value of fractal dimension was almost constant during the whole immersion time. And the fractal dimensions *D* of general corrosion and passivation were 2.411 and 2.242 respectively, which were larger than 2. But for pitting corrosion and crack propagation, the fractal dimensions were 1.540 and 1.001 respectively, which were much lower than 2. The average fractal dimension value for intergranular corrosion was 1.970 (around 2). It was concluded that the *D* value was decreased in the order of general corrosion, passivation, intergranular corrosion, pitting corrosion and crack propagation.

4. DISCUSSIONS

It is well known that the corrosion phenomenon is caused by the micro cells formed on the electrode surface, and their distribution determines the attacked morphology.[15] EN is characterized by the random fluctuation of the current/potential arising from micro cells, hence different EN characteristics will represent distinct electrode activities.[6]

General corrosion is defined as uniform thinning [33]. It processes with numerous alternate micro-anodic/ micro-cathodic reactions on the whole electrode area, the quantity of dissolved material and the depth of corrosion are almost the same on the whole metal surface (Fig. 1a) [8]. Passivation of stainless steel means a thin passive film forms on the metal surface, and the corrosion rate of metal is

greatly reduced (Fig. 1b) [34, 35]. The common characteristics of general corrosion and passivation are the electrochemical behaviors occur uniformly on the whole electrode area, and along with corrosion depth or film thickness in the vertical direction. In general, it is expected that high frequency events tend to occur all over the surface, while low frequency corrosion events exist in individual locations with removing relatively large amounts of material.[10, 36] So the EN signals under general corrosion and passivation are mainly in white noise signals with high frequency (Fig. 2a and 2b, Fig. 3a and 3b) and thus the low slope value of β (Fig. 4a and 4b). The fractal dimensions D of general corrosion and passivation are larger than 2 (2.411 for general corrosion and 2.242 for passivation) (Fig. 5), which are in agreement with the dimensions of attacked morphology shown in Fig. 1a and 1b.

The fractal dimension D of general corrosion (2.411) is larger than that of passivation (2.242), which probably indicates that the corrosion depth of general corrosion is larger than the thickness of the passive film formed on the metal.[37]

Pitting corrosion is always occurred in localized areas due to the breakdown of passive film and the attack of corrosive ions like Cl^- .[33] Stress corrosion cracking often origins from the surface defects or pitting, and the crack propagation is taken place in the crack tip.[38] The common characteristics of pitting corrosion and crack propagation are the existence of small anodic reaction areas (the fresh metal in pits or crack tip) and large cathodic areas (the rest metal surface). These localized corrosion processes should have low frequency EN signals (Fig. 2d and 2e, Fig. 3d and 3e) and a large slope value of β (Fig. 4d and 4e). The fractal dimension of pitting corrosion is 1.540 and crack propagation is around 1.001, which implies that the materials dissolve at the localized locations (Fig. 1d and 1e).

Intergranular corrosion is a kind of localized attack,[28] and the preferential anodic dissolution takes place at the grain boundaries while the interior of the grains remains passive under certain electrochemical conditions.[39] It is clearly that intergranular corrosion occurs more uniformly on metal surface than pitting, whereas less uniformly than general corrosion (Fig. 1c). So the slope β and fractal dimension value D (1.970) of intergranular corrosion is between those of general corrosion and pitting corrosion, as shown in Fig. 4 and Fig. 5.

From the above results, it can be concluded that the EN signals under different corrosion types have the distinct fluctuation frequency, power slope β value and fractal dimension D. So the fractal dimension D calculated by wavelet transform can be a useful parameter to discriminate the corrosion types of 304 SS, and evaluate the localized degree of corrosion.

5. CONCLUSIONS

1) Under general corrosion and passivation of 304 SS, the EN signals have high frequency and low power slope β. The fractal dimensions are larger than 2.

2) The fractal dimensions of pitting corrosion and crack propagation during SCC of 304 SS are much lower than 2, and the fractal dimension of intergranular corrosion is around 2.

3) The fractal dimension D can be used as a novel parameter to distinguish the corrosion type of materials, and evaluate the localized degree of corrosions.

ACKNOWLEDGEMENTS
This paper was supported by National Key Basic Research Program of China (No.2011CB610505).

References

1. H. Shaikh, R. Amirthalingam, T. Anita, N. Sivaibharasi, T. Jaykumar, P. Manohar, H. S. Khatak, *Corros. Sci.*, 49 (2007) 740.
2. C. Hu, S. Xia, H. Li, T. Liu, B. Zhou, W. Chen, N. Wang, *Corros. Sci.*, 53 (2011) 1880.
3. J. Xu, X. Q. Wu, E.-H. Han, *Corros. Sci.*, 53 (2011) 448.
4. F. Mohammadi, T. Nickchi, M. M. Attar, A. Alfantazi, *Electrochim. Acta*, 56 (2011) 8727.
5. A. Arutunow, K. Darowicki, *Electrochim. Acta*, 53 (2008) 4387.
6. D. Xia, S. Song, J. Wang, J. Shi, H. Bi, Z. Gao, *Electrochem. Commun*., 15 (2012) 88.
7. P. Planinšič, A. Petek, *Electrochim. Acta*, 53 (2008) 5206.
8. X. Jiang, S. Nešić, F. Huet, B. Kinsella, B. Brown, D. Young, *J. Electrochem. Soc*., 159 (2012) C283.
9. K. Sasaki, H. S. Isaacs, *J. Electrochem. Soc.*, 151 (2004) B124.
10. H. A. A. Al-Mazeedi, R. A. Cottis, *Electrochim. Acta*, 49 (2004) 2787.
11. J. M. Sanchez-Amaya, R. A. Cottis, F. J. Botana, *Corros. Sci*., 47 (2005) 3280.
12. T. Anita, M. G. Pujar, H. Shaikh, R. K. Dayal, H. S. Khatak, *Corros. Sci*., 48 (2006) 2689.
13. Y. Y. Shi, Z. Zhang, F. H. Cao, J. Q. Zhang, *Electrochim. Acta*, 53 (2008) 2688.
14. J. J. Kim, *Mater. Lett.*, 61 (2007) 4000.
15. E. García-Ochoa, F. Corvo, *Electrochem. Commun*., 12 (2010) 826.
16. A. Legat, V. Doleček, *J. Electrochem. Soc*., 142 (1995) 1851.
17. X. F. Liu, H. G. Wang, H. C. Gu, *Corros. Sci*., 48 (2006) 1337.
18. R. Chen, V. Trieu, H. Natter, J. Kintrup, A. Bulan, R. Hempelmann, *Electrochem. Commun*., 22 (2012) 16.
19. A. M. Homborg, T. Tinga, X. Zhang, E. P. M. van Westing, P. J. Oonincx, J. H. W. de Wit, J. M. C. Mol, *Electrochim. Acta*, 70 (2012) 199.
20. A. Aballe, M. Bethencourt, F. J. Botana, M. Marcos, *Electrochim. Acta*, 44 (1999) 4805.
21. A. Aballe, M. Bethencourt, F. J. Botana, M. Marcos, *Electrochem. Commun*., 1 (1999) 266.
22. J. A. Wharton, R. J. K. Wood, B. G. Mellor, *Corros. Sci*., 45 (2003) 97.
23. M. Shahidi, S. M. A. Hosseini, A. H. Jafari, *Electrochim. Acta*, 56 (2011) 9986.
24. Z. Dong, X. Guo, J. Zheng, L. Xu, *Electrochem. Commun*., 3 (2001) 561.
25. J. M. Costa, F. Sagués, M. Vilarrasa, *Corros. Sci*., 32 (1991) 665.
26. S. Girija, U. K. Mudali, V. R. Raju, R. K. Dayal, H. S. Khatak, B. Raj, *Mater. Sci. Eng*., A, 407 (2005) 188.
27. M. Gomez-Duran, D. D. Macdonald, *Corros. Sci*., 45 (2003) 1455.
28. S. Jain, N. D. Budiansky, J. L. Hudson, J. R. Scully, *Corros. Sci*., 52 (2010) 873.
29. J. R. Kearns, J. R. Scully, P. R. Roberge, D. L. Reichert, J. L. Dawson, Electrochemical Noise Measurement for Corrosion Applications. ASTM Publication, West Conshohocken (1996).
30. Y. Shi, Z. Zhang, J. Su, F. Cao, J. Zhang, *Electrochim. Acta*, 51 (2006) 4977.
31. M. Attarchi, M. S. Roshan, S. Norouzi, S. K. Sadrnezhaad, A. Jafari, *Journal of Electroanalytical Chemistry*, 633 (2009) 240.
32. F. H. Cao, Z. Zhang, J. X. Su, Y. Y. Shi, J. Q. Zhang, *Electrochim. Acta*, 51 (2006) 1359.
33. C. Jirarungsatian, A. Prateepasen, *Corros. Sci*., 52 (2010) 187.
34. K. Darowicki, A. Mirakowski, S. Krakowiak, *Corros. Sci*., 45 (2003) 1747.
35. U. Kamachi Mudali, Y. Katada, *Electrochim. Acta*, 46 (2001) 3735.
36. K.-H. Na, S.-I. Pyun, *Corros. Sci*., 50 (2008) 248.

37. H. Luo, C. F. Dong, K. Xiao, X. G. Li, *Applied Surface Science*, 258 (2011) 631.
38. J. C. Lin, H. L. Liao, W. D. Jehng, C. H. Chang, S. L. Lee, *Corros. Sci*., 48 (2006) 3139.
39. A. Abou-Elazm, R. Abdel-Karim, I. Elmahallawi, R. Rashad, *Corros. Sci*., 51 (2009) 203.